Processing of Short-Fiber Reinforced Polypropylene. I. Influence of Processing Conditions on the Morphology of Extruded Filaments

SILVIA E. BARBOSA* and JOSÈ M. KENNY**

*PLAPIQUI (UNS-CONICET) CC 717
(8000) Bahía Blanca-Argentina

**Institute of Chemical Technologies
University of Perugia
Terni, Italy

An experimental investigation of the processing of glass fiber reinforced polypropylene is presented. Final fiber orientation distribution, fiber distribution in filament sections, rheological properties, final fiber length distribution and surface morphology were analyzed. This analysis was done taking into account the quantity of fibers and their interactions and flow conditions. The final fiber orientation increased when shear rate increased and fiber concentration decreased. Moreover, inhomogeneities in fiber distribution increased as the concentration of fibers decreased. The density profile showed a significant variation with fiber concentration, but it was not dependent on the shear rate applied. The viscosity showed a linear dependence with shear rate. The average fiber length and the breadth of this distribution decreased with the increasing fiber concentration and extrusion rate. The extruded filament surface showed minor roughness when the shear rate increased or when the fiber concentration decreased. The results of this experimental characterization give useful information to determine the influence of the processing variables on the final properties of short-fiber reinforced polypropylene and constitutes the first part of a more ambitious project that also includes the development of a modeling strategy of the processing behavior for short-fiber composites.

INTRODUCTION

Short-fiber reinforced thermoplastics are very important commercial materials. Whereas good processability is typical of short-fiber composites, the mechanical properties of the final products mainly depend on the residual fiber length, orientation and distribution which are determined by the processing conditions. The ability to predict and control the fiber fragmentation, orientation and distribution in the processed part depends on the accuracy of the rheological description of these materials and on the ability to simulate their flow behavior. In fact, not only the viscosity of the composite system depends on the processing conditions and on the characteristics of the fibers, but, at the same time, the residual length and orientation are strongly affected by the material viscosity (1–6). Thus, the formulation of useful rheological models requires the characterization of the polymeric composites under simple conditions where the effects of the different variables can be uncoupled. In this regard, the behavior of model suspensions with Newtonian or well characterized non-Newtonian matrices (7–9) has been reported.

In recent years, Goettler (10) working with thermoset matrix, found a quantitative relationship between orientation distribution and mechanical properties. Bright *et al.* (11) studied the rheological properties of reinforced polymers in a capillary rheometer and found that at low shear rates, fibers cause a significant increase of the viscosity, but at high shear rates the filled and unfilled melts have very similar viscosities which follow the power law model. Czarnecki *et al.* (12) studied rheological properties, fiber damage and mastication characteristics of polystyrene melts reinfoced with aramid, glass and cellulose fibers. They worked with a rotational rheometer at low shear rates and found that the addition of fibers increases the

*To whom correspondence should be addressed.

viscosity in the same manner as a reduction in temperature; then data may be superposed by reduced plotting. Knutsson *et al.* (13) studied the rheological and extrusion characteristics of glass fiber-reinforced polycarbonate. They found a similar shear rate dependence of the viscosity measured in cone-plate and capillary rheometers. The presence of fibers increases the level of viscosity, decreases the extrudate swell and increases the surface roughness. Bercraft *et al.* (14) reported experimental measurements of rheology, morphology and flow characteristics of short-fiber reinforced thermoplastics. They used the Doi-Doraiswamy equations for rigid rod suspensions for the interpretation of their results.

The research presented here deals with polymeric systems similar to those reported in previous publications (11–14). However, in this work, a model system with monodisperse fibers has been adopted allowing a more accurate analysis of fiber interactions that can lead to the decoupling of damaging effects that in this case can only be attributed to the extrusion process.

As a first step in the general objective of analyzing the processability of thermoplastic matrix short-fiber composites a careful analysis of their rheological behavior is required. In our research the characterization of polypropylene reinforced with short glass fibers has been performed on an extruder provided with a rheometric die. Different variables have been considered: fiber concentration, rotational speed and capillary geometry. The experimental results are presented in terms of material viscosity, filament morphology and fiber orientation and distribution. The rheological characterization of fibrous multiphase systems under controlled orientation conditions and the development of phenomenological models represent very important preliminary steps to allow a better understanding of the flow behavior of these materials in real processing conditions and complex geometries.

EXPERIMENTAL

Materials

The material used in this research was glass fiber reinforced polypropylene. Moplen 20 polypropylene (injection grade) kindly supplied by Himont (currently Montell) in powder form was used as matrix. Short glass fibers Vetrotex EC5168, polypropylene compatible, supplied in the form of chopped strands of about 100 fibers each were used at different concentrations. Fiber dimensions before processing were 4.5 mm in length and 13 μm in diameter.

Equipment and Measurements

Compounding: Different proportions of the powder resin and the chopped strands of fibers were mixed mechanically to prepare compounds with different fiber weight concentrations. These compounds were processed in a Haake single screw extruder (ϕ = 19 mm) with a rheometric capillary die. Five different fiber weight fractions—0, 5, 10, 20 and 30 wt% named C0, C5, C10, C20, C30, respectively, were prepared and tested. All the samples were analyzed using four capillaries of 1.2 mm in diameter with different lengths to diameter ratios: 10, 20, 30 and 40. Several barrel rotation velocities were adopted in order to cover a range of shear rate of practical interest for composite processing. Typical barrel and die temperature profiles were used (180°C-200°C-220°C-220°C-230°C) and kept constant during extrusion.

Glass fiber concentration after processing was determined by weight difference after ashing extruded samples in a convection oven at 450°C for 5 hours. This analysis was repeated for all fiber concentrations, in all the extrusion conditions. The difference observed compared to the nominal fiber concentration before extrusion was less than 4% in all the samples. The analysis of the strands disintegration was made by direct observation of the ashed residuals. Final fiber lengths were measured by image analysis of more than 2000 fragments in each ashed sample.

Morphology analysis: The surface roughness and cross sections of the extruded filaments were analyzed by scanning electronic microscope SEM-Cambridge 2000. Cross sections of specimens, obtained by fracturing extruded filaments in liquid nitrogen, were observed by SEM.

Methodology of filament section analysis. Image analysis was also performed on scanned SEM microphotographs. From the center of the sections six concentric annular regions of thickness = 100 μm were defined and analyzed. The area covered by fibers was then computed and corrected for fiber orientation changes. To minimize the error, several enlarged areas were analyzed. Fiber concentration in the sections was then determined as the ratio of the areas. Fiber orientation was determined by evaluation of the major axis of the ellipses corresponding the fiber cross section (11, 12). All the results were reported as a function of the distance from the filament center.

RESULTS AND DISCUSSION

Rheological Properties

Experimental data of the rheological behavior of the compounds were analyzed with the typical corrections used in capillary rheometry: Rawinowich equation for non-Newtonian behavior and Bagley correction for entrance and exit turbulence effects (15). *Figure 1* shows corrected viscosity vs. shear rate curves of the pure polypropylene and of compounds with different glass fiber content. The shear-thinning behavior is observed. Although, a marked effect of fiber concentrations is expected in all of the range of shear rate tested, this effect can be observed only at low shear rates. Fiber contribution to suspension viscosity is masqueraded by the behavior of neat matrix and by the fiber orientation distribution. At low shear rates, fibers are not all oriented in flux lines, then they contribute more to the suspension viscosity because the

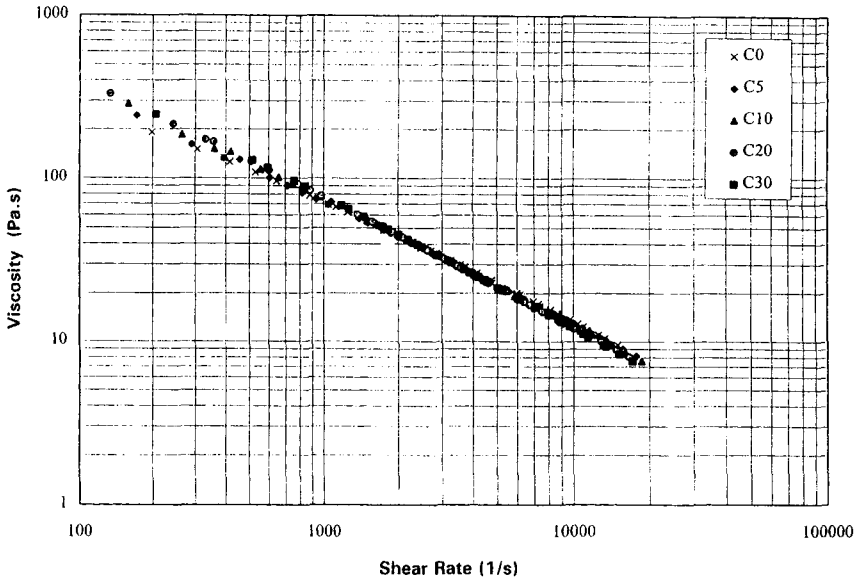

Fig. 1. Shear viscosity vs. shear rate of PP compounds with different glass fiber contents: 0, 5, 10, 20, 30 wt%.

area that they oppose to the flux is greater. When the shear rate increases, the convergent flow induces the orientation of the majority of the fibers in the flow direction. Then, the contribution of the fibers to the suspension viscosity becomes smaller because the section exposed to the flux is reduced. The relation between fiber orientation distribution and the shear rate is analyzed below.

The results of the experimental characterization have been analyzed using different simple rheological models: Casson, power law, linear model with two parameters (Bingham) and Herschel-Bulkey equation with three parameters. In our case the best fitting was obtained with the power law equation:

$$\tau = k(\dot{\gamma})^n \Rightarrow \eta = k(\dot{\gamma})^{n-1} \quad (1)$$

where η is the shear viscosity, τ is the shear stress, $\dot{\gamma}$ is the shear rate, k is the consistency and n is the power law index. *Table 1* shows the power law parameters computed for the different compounds. The consistency increases and the power index decreases with fiber content. These observations are in agreement with earlier studies (11–14). It is interesting to notice that the power law model does a better job simulating the composite viscosity than the matrix viscosity.

Table 1. Rheological Parameters of the Glass Fiber Reinforced Polypropylene Compounds Studied.

Fiber Concentration	Viscosity	
wt%	k (Pa.s^{-n})	n
0	9357	0.30
5	11083	0.27
10	11925	0.26
20	13787	0.25
30	16959	0.21

Morphology of Extruded Filaments

Irregularities in the extrudates morphology were observed as a function of the fiber concentration and processing conditions. *Figure 2* shows microphotographs of the skin of filaments obtained at 40 rpm of screw speed ($\dot{\gamma} \sim 2000$ 1/s) and with a capillary die of L/D = 30. In a comparative analysis it can be observed that irregularities increase with the glass fiber content while the surface of neat PP is regular and continuous. For high fiber contents, the fibers protruded from the surface of the filaments, generating a large number of superficial voids and craters. There was no significant influence of the capillary length on these results in a limited range of shear rates.

Figure 3 shows microphotographs of filaments of composites with 20 wt% fiber content extruded with different screw speeds (5 rpm-$\dot{\gamma} \sim 200$ 1/s, and 90 rpm-$\dot{\gamma} \sim 4500$ 1/s), which should also be compared with *Fig. 2d* obtained for the same material (40 rpm-$\dot{\gamma} \sim 2000$ 1/s). It can be observed that at low shear rates, many fibers protruded from the surface of the filaments, and there is a low surface fiber orientation. As the shear rate increases, the superficial fibers are more aligned and the surface is more regular. On the other hand, a very good fiber-matrix adhesion was observed in all the microphotographs, indicating a good fiber wettability.

Fiber-Fiber Interaction Analysis

The above observations can be interpreted in terms of fiber-fiber interactions. In fact, the processing of a short-fiber composite material can be studied in terms of the flow of a fiber suspension in a neat resin. Fiber suspensions can be classified into three categories as a function of the fiber concentration: dilute, semi-concentrated and concentrated. In a dilute regime each fiber is a free buoyancy particle and its movements are not influenced by the other ones. On the other

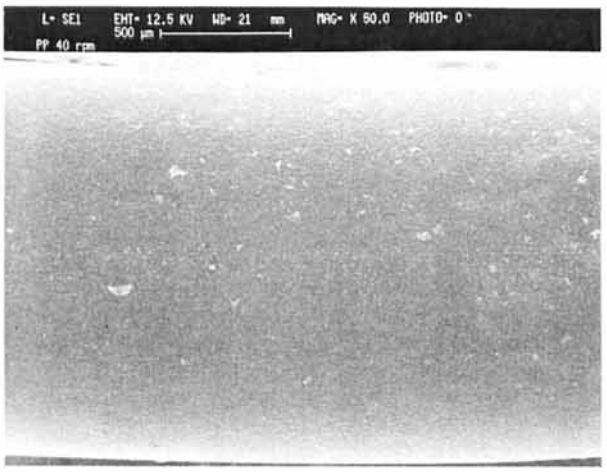

(a)

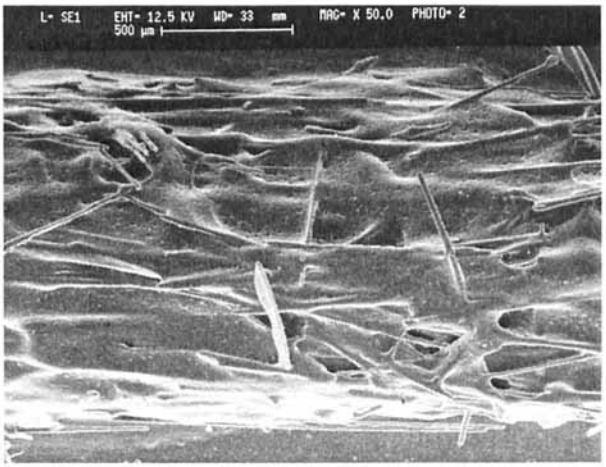

(d)

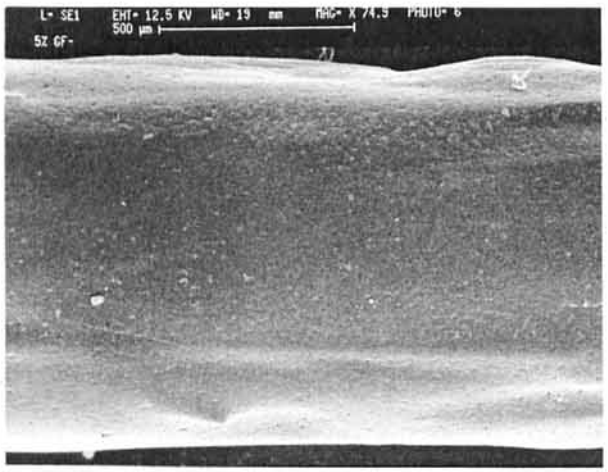

(b)

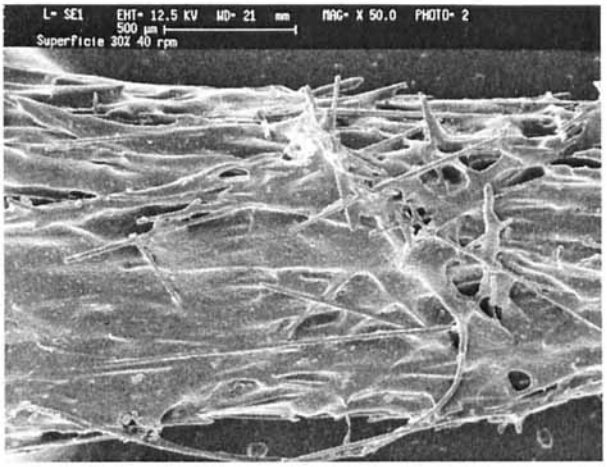

(e)

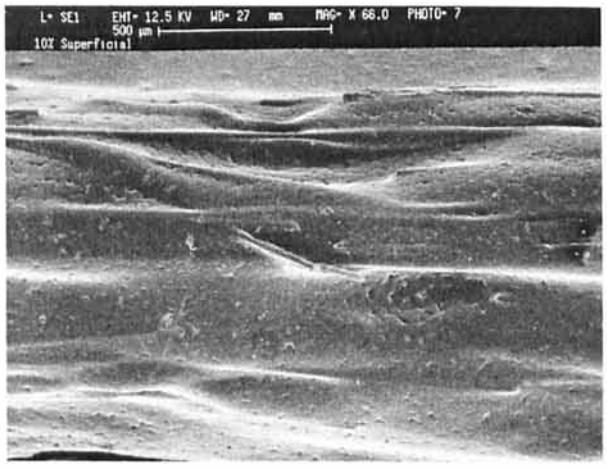

(c)

Fig. 2. SEM microphotographs of the surface of filaments of PP compounds extruded at 40 rpm. a) Neat PP; b) 5 wt% glass fiber; c) 10 wt% glass fiber; d) 20 wt% glass fiber; e) 30 wt% glass fiber.

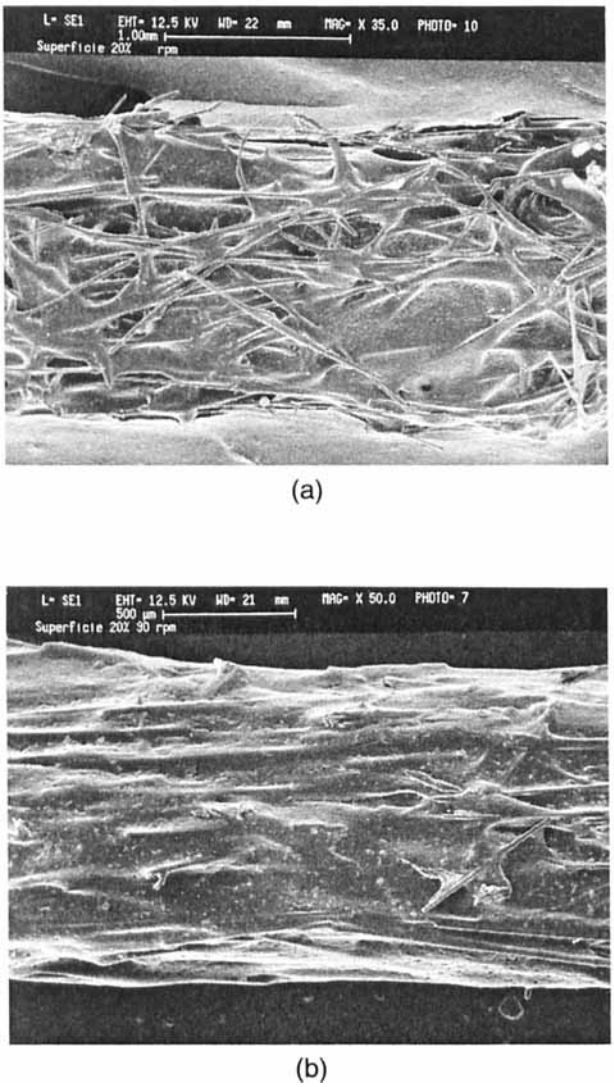

Fig. 3. SEM microphotographs of the surface of 20 wt% glass fiber filled PP filaments extruded at different screw speeds: a) 5 rpm; b) 90 rpm.

Table 2. Parameter nL^3 for Different Glass Fiber Reinforced Polypropylene Composites.

Concentration (wt%)	nL^3
5	172
10	344
20	688
30	1031

hand, in a concentrated suspension, the quantity of fibers is high enough for the suspension to behave like a solid. Intermediate concentrations where the interaction of fibers is important correspond to the semiconcentrated regime.

Weight or volume fraction are the parameters most widely used for describing suspension concentration. These parameters can properly describe the concentration of spherical particles; however, in the case of fiber suspensions where one particle dimension is very different from the others, these parameters can be meaningless when used alone. For a given fiber weight or volume fraction the spacing between fibers depends on the fiber aspect ratio (L/D) and on the fiber orientation distribution. Then, there is a more useful parameter to describe fiber suspensions: nL^3 (16–19). This quantity expresses the number of fibers in the domain swept out by a fiber rotating about its minor axis. Its relation with the weight fraction is given by:

$$nL^3 = \phi_w \frac{\rho_m}{\rho_f}\left(\frac{L}{D}\right)^2 \frac{4}{\pi} \tag{2}$$

where ϕ_w is the weight fraction of fibers, n is the number of fibers in a volume unit, D is the fiber diameter, L is the fiber length and m and f are respectively matrix and fiber density.

In terms of nL^3 the limits for a semiconcentrated suspension are (18):

$$1 < nL^3 < L/D \quad \text{for a random fibers orientation system} \tag{3}$$

$$1 < nL^3 < (L/D)^2 \quad \text{for an aligned fibers orientation system} \tag{4}$$

Inside the regions defined by *Eq 3* and *4* fiber-fiber interactions are relevant. The parameter nL^3 was calculated for all the suspensions studied using *Eq 2*. The value of L/D = 150 was used as the average of the final length values measured. Polypropylene melt density (0.75 g/cm^3) was computed at 230°C using the Hartman-Haake equation (20). Glass density was taken equal to 2.57 g/cm^3. *Table 2* shows the values of nL^3 for the different weight fraction composites. Taking into account that this is a convergent flow, the fiber orientation distribution obtained is characteristic of an aligned system. Then, the limits for semiconcentrated suspensions can be calculated using *Eq 4*: $1 < nL^3 < 22{,}500$. The values of nL^3 reported in *Table 2* show that all the suspensions used are semiconcentrated and because of that fiber-fiber interactions should play a very important role in their flow behavior.

The concepts expressed above can explain the observations regarding the increasing disorder in the composite surfaces as the fiber concentration increases. In fact, the surface of the low concentrations sample (5%) is smoother than that of the 30% compound. In the first case, following *Table 2*, when a fiber rotates it can interact with another 206 fibers, but when the weight concentration is 30% the interaction possibilities are 6 times higher.

Fiber Concentration Distribution in Filament Sections

Figure 4 shows microphotographs of filament sections of a 20 wt% glass fiber compound extruded at three different screw speeds: 5 rpm ($\dot{\gamma} \sim 200$ 1/s), 40 rpm ($\dot{\gamma} \sim 2000$ 1/s) and 90 rpm ($\dot{\gamma} \sim 4500$ 1/s). At first

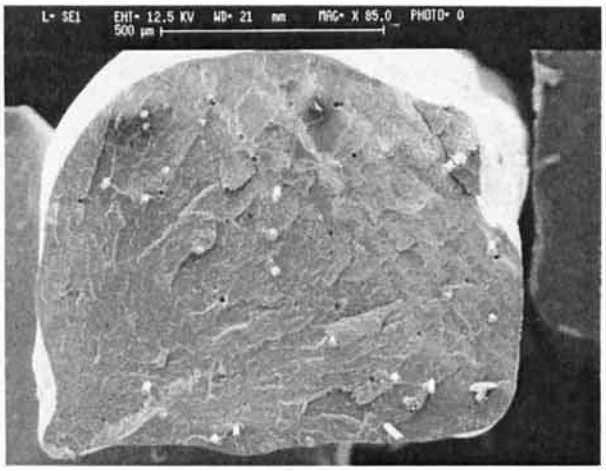

(a)

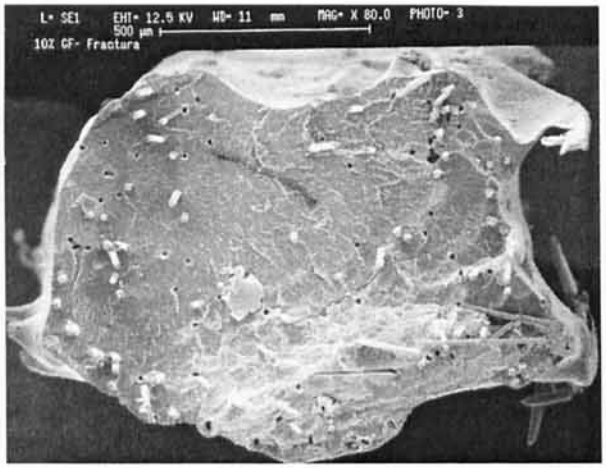

(b)

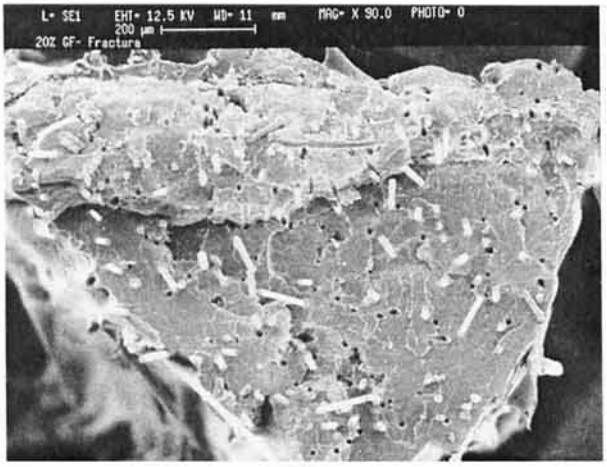

(c)

Fig. 4. SEM microphotographs of extrudate filament fracture sections of 20 wt% glass fiber filled PP filaments extruded at different screw speeds: a) 5 rpm, b) 40 rpm and c) 90 rpm.

sight it is possible to observe that the irregularities of the surface reported above influence the quality of the section, which also in this case increases with the shear rate and decreases with the fiber concentration. However, the most important information obtained from the filament sections concerns fiber concentration distribution, which, in a first view, seems to vary with the section radius with a higher fiber concentration on the borders.

Following the method described in the **Experimental** section an accurate determination of the homogeneity of the fiber concentration was performed. The values of local fiber concentration were normalized using the average concentration value of the whole filament section. *Figure 5* shows these results as a function of the section radius for different fiber concentration compounds prepared at 40 rpm ($\dot{\gamma} \sim 2000$ 1/s). In order to perform a comparative analysis, the velocity profiles were calculated and plotted in the same figure. In all cases, the fiber concentration increases from the filament center to the borders. As expected, fibers tend to move away to zones characterized by high velocity gradients. It is also observed that the homogeneity of the fiber concentration distribution increases with the fiber concentration as a consequence of the reduced fiber mobility and increased fiber-fiber interaction.

The influence of the shear rate on the fiber concentration distribution is reported in *Fig. 6* which shows dimensionless concentration and velocity profiles for the 20 wt% glass fiber polypropylene compound processed at three different screw speeds (5 rpm-$\dot{\gamma} \sim 200\ s^{-1}$, 40 rpm-$\dot{\gamma} \sim 2000\ s^{-1}$ and 90 rpm-$\dot{\gamma} \sim 4500\ s^{-1}$). For the three conditions the fiber concentration profiles are similar indicating that the radial migration of the fibers is not controlled by the shear rate in the interval studied. Under the experimental conditions used in this research, corresponding to those of typical extrusion and injection molding processes, the fiber concentration distribution is already fixed and no more fiber migration is produced by a further increase of the shear rate.

Fiber Orientation Distribution

The fiber orientation distribution is typically described through the orientation function which is defined in terms of the orientation angle (α) of the fiber with respect to the flow direction:

$$f = \langle \cos\alpha \rangle^2 \tag{5}$$

where:

$$\langle \cos\alpha \rangle = \sum_{i=1}^{n} \frac{\cos\alpha_i}{n} \tag{6}$$

The extreme values of this function are: $f = 1$, which means optimum alignment, and $f = 0$ obtained when all the fibers are perpendicular to the flow direction. Intermediate values can be obtained in a real case.

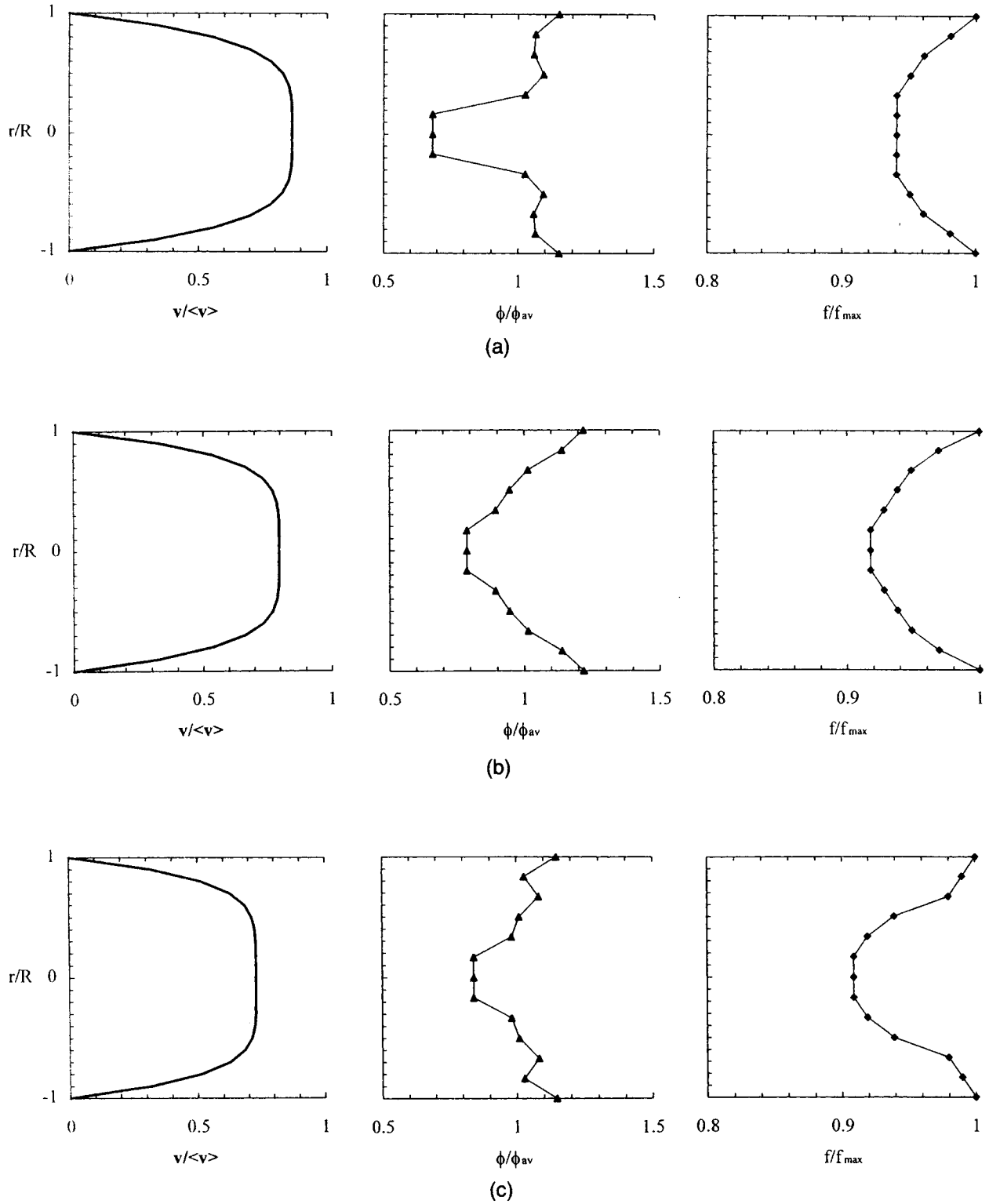

Fig. 5. Velocity, density and orientation profiles for glass fiber filled PP prepared at 40 rpm screw speed and with different fiber concentrations: a) 5 wt%, b) 10 wt%, c) 20 wt% and d) 30 wt%.

The method described in the **Experimental** section was used to evaluate α, and then, f was computed for the different sections analyzed. The experimental results, normalized with the maximum value obtained, are reported in *Fig. 5* as a function of the dimensionless capillary radius and compared with the velocity profiles

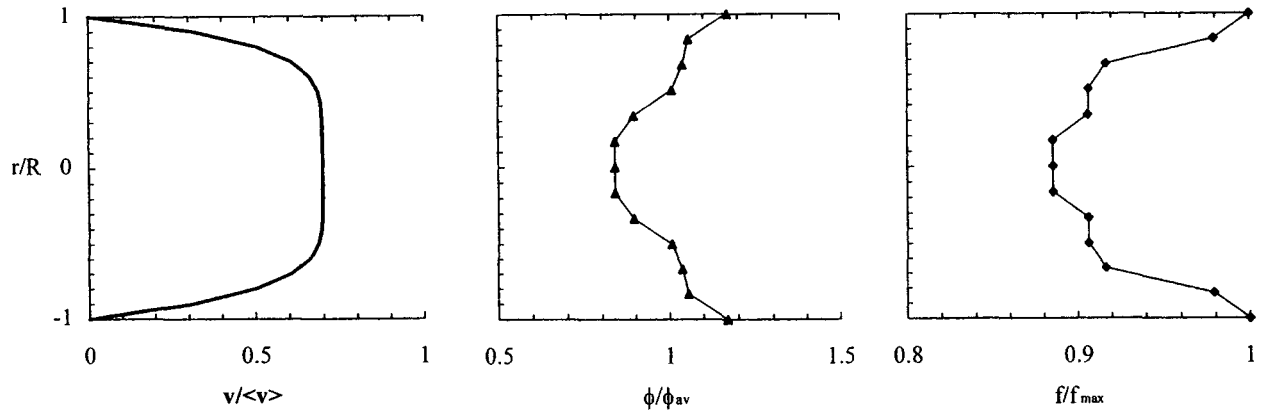

(d)

Fig. 5. Continued.

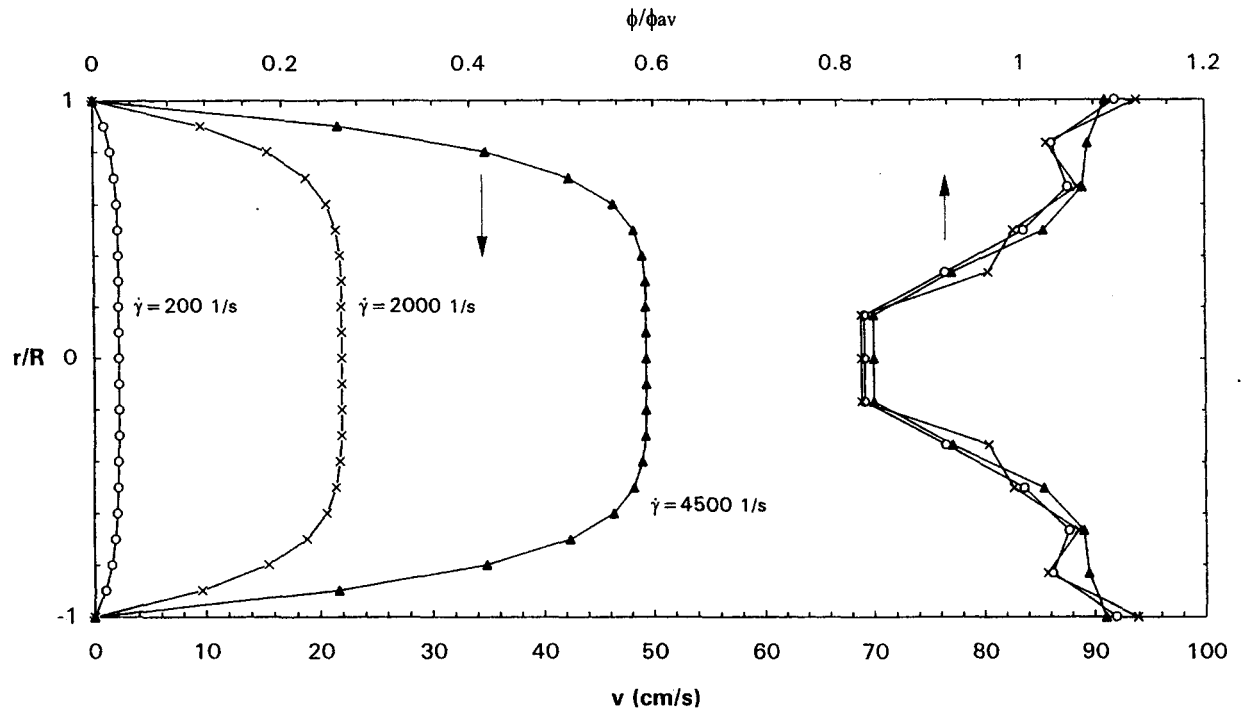

Fig. 6. Velocity and density profiles for 20 wt% glass fiber filled PP extruded at different screw speeds: 5 rpm, 40 rpm and 90 rpm.

and fiber concentration results already discussed. High orientation values were obtained and they increase from the center to the skin of the filaments. This behavior is characteristic of extrusion dies where the flow is strongly convergent (21). The values of f obtained around the center of the capillary, where the flow is only elongational were independent of length. The suspension fiber orientation distribution was measured before entering the die, and f values were the same order that those measured in the center of the die. This effect was expected because in the zone around the center of the capillary the flux is slight perturbed (ideally there are not perturbations in the center line of the capillary). The orientation function also increases when concentration decreases as a consequence of the reduced fiber-fiber interactions.

Figure 7 shows dimensionless orientation distribution and velocity profiles for the 20 wt% glass fiber polypropylene compound extruded at three different screw speeds, 5, 40 and 90 rpm, ($\dot{\gamma} \sim 200$, 2000 and 4500 s^{-1}). Fiber orientation increases and it is more uniform as the shear rate increases.

A further insight into the fiber orientation behavior was obtained by analyzing the filament ashing residues. It was observed that short-fibers generate a very intricate mat, which can be handled without breaking. In

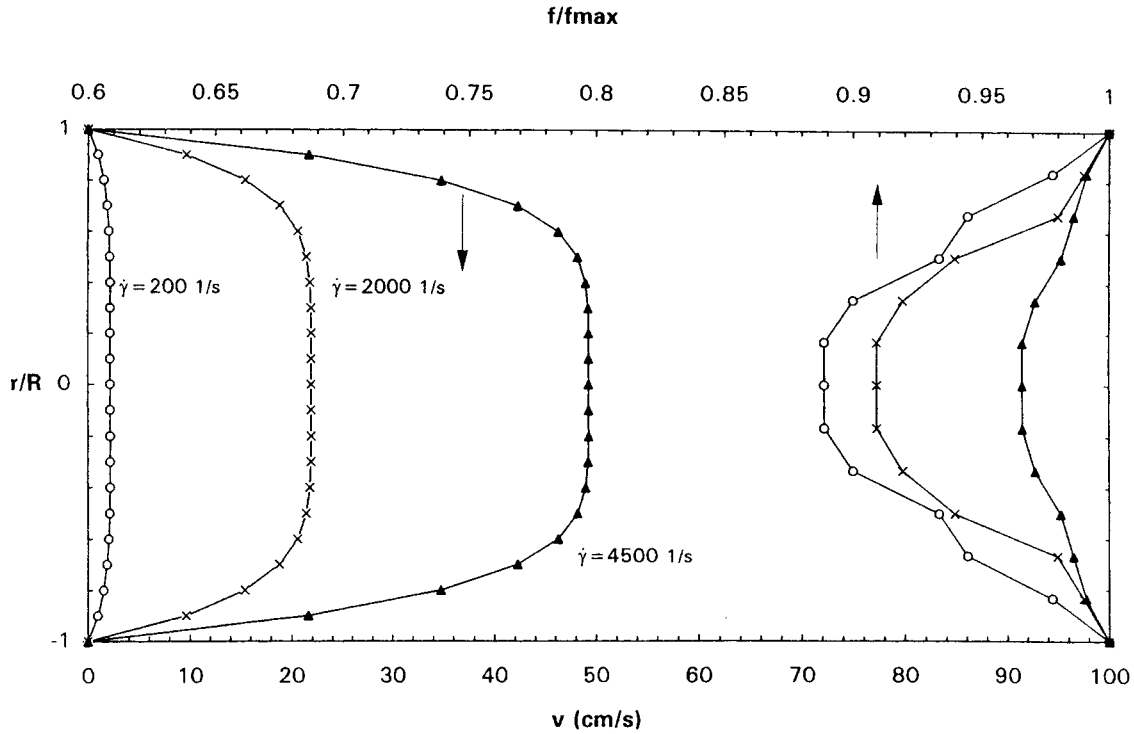

Fig. 7. Velocity and orientation profiles for 20 wt% glass fiber filled PP extruded at different screw speeds: 5 rpm, 40 rpm and 90 rpm.

terms of surface fiber orientation, the observations regarding this analysis confirm the results obtained above.

Effects of the Presence of Fibers on the Flow Behavior

The flow of fiber suspensions is mainly affected by the rigidity and the orientation of the suspended fibers (20). In a homogeneous velocity field, the center of mass of a fiber moves affinely with the bulk, but each fiber point has a different velocity as a consequence of the fiber rigidity. This velocity gradient generates stresses that induce forces over the fibers originating different changes in the properties of suspensions. In a homogeneous shear field it has been demonstrated (17, 18) that the induced force on the fiber (F) is proportional to the shear rate ($\dot{\gamma}$) and to the viscosity of the suspending medium (η_s), and is also a function of the fiber orientation vector (**p**), the aspect ratio (L/D) and the fiber interspersing (h). It should be noticed that the last one is a dynamic function of **p** and depends on the fiber-fiber interaction. Summarizing:

$$\mathbf{F} \propto \eta_s, \dot{\gamma}, f(L/D, h, \mathbf{p}) \quad (7)$$

The linear relationship between **F** and $\dot{\gamma}$ has been demonstrated (18) for suspensions in a Newtonian

Table 3. Parameters of Fiber Length Distributions for Composites of Different Fiber Contents Prepared at 40 rpm Screw Speed in a Capillary Die of 36 mm Length (L/D = 30).

Conc. (wt%)	L_n (mm)	L_w (mm)	P
5	2.31	2.90	1.28
10	2.10	2.79	1.33
20	1.80	2.43	1.35
30	1.30	2.21	1.70

Table 4. Parameters of Fiber Length Distributions for Composites With 20 wt% Glass Fiber Content Prepared at 40 rpm Screw Speed With Capillaries of Different Lengths.

L/D Die Ratio	L_n (mm)	L_w (mm)	P
10	1.40	1.82	1.30
20	1.27	1.69	1.33
30	1.30	2.21	1.70
40	1.32	1.98	1.50

Table 5. Parameters of Fiber Length Distributions for Composites with 20 wt% Glass Fiber Content Prepared in a Capillary Die of 36 mm of Length (L/D = 30) at Different Screw Speeds.

Extrusion Rate (rpm)	Shear Rate (s^{-1})	L_n (mm)	L_w (mm)	P
5	176	2.05	2.87	1.40
40	2117	1.30	2.21	1.70
90	4412	1.10	2.03	1.85
120	5825	1.11	1.89	1.70
180	8560	0.70	1.42	2.03

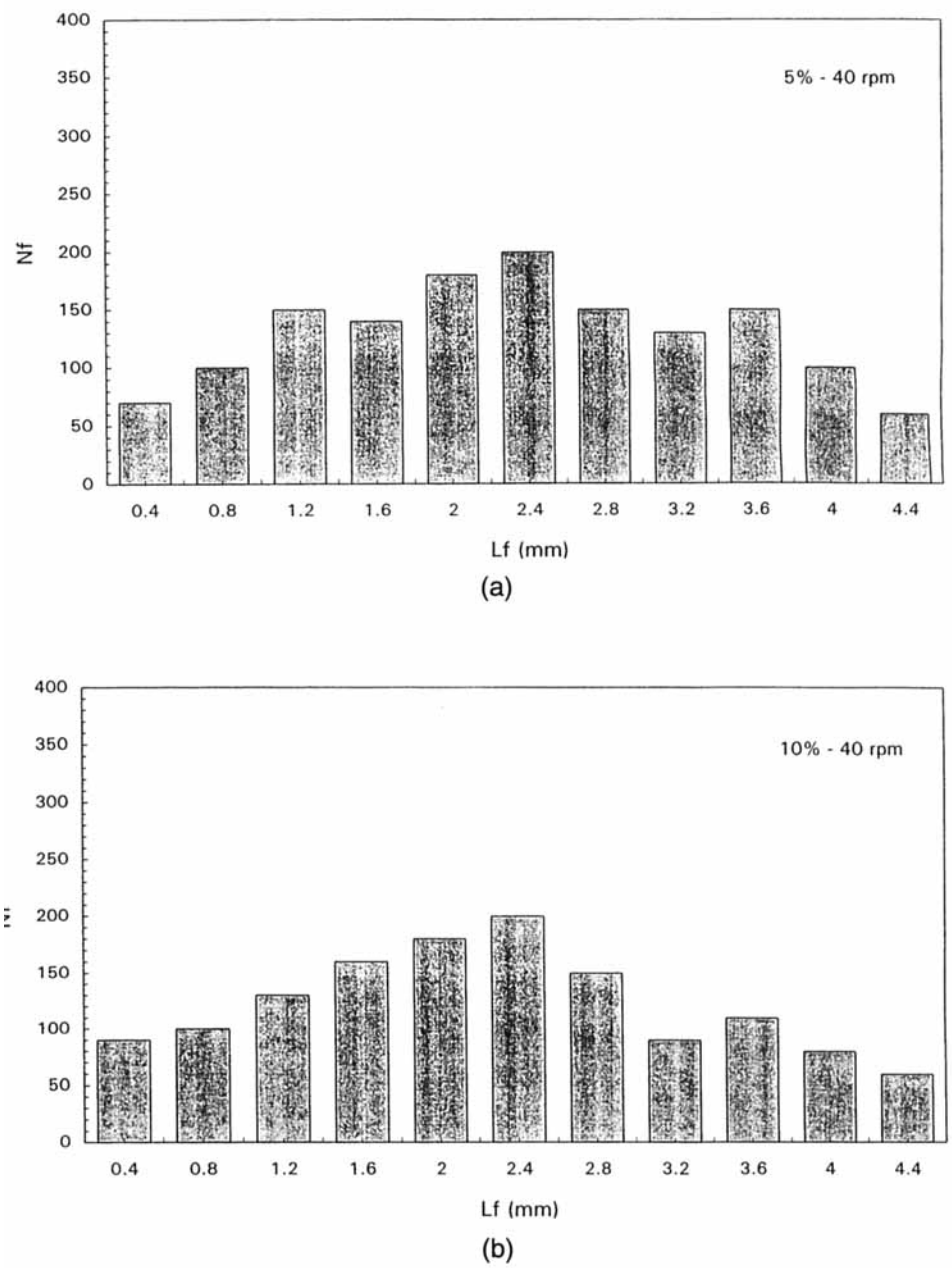

Fig. 8. Final fiber length distribution histograms for glass fiber filled PP prepared at 40 rpm screw speed and with different fiber concentrations: a) 5 wt%; b) 10 wt%; c) 20 wt%; d) 30 wt%.

matrix ($\eta_s \neq \eta_s(\dot{\gamma})$). In a shear thinning solvent there is an additional and opposite contribution to the force originated in the variation of the matrix viscosity with the shear rate. The experimental results obtained in this research, which show the increase of fiber alignment with the shear rate, indicate that the second effect is more important than the first one. In fact, *Eq 7* for a suspension in a power law matrix becomes:

$$\mathbf{F} \propto \dot{\gamma}^n, f(L/D, h, \mathbf{p}) \quad (8)$$

As $n > 0$, the net effect of the increase of the shear rate is an increase of the net force that aligns the fiber in the flow field.

Final Fiber Length

Following the technique described in the **Experimental** section, fibers were separated from the matrix by ashing and their length was measured. The fiber length distribution was then determined statistically using a method of moments (14) similar to those

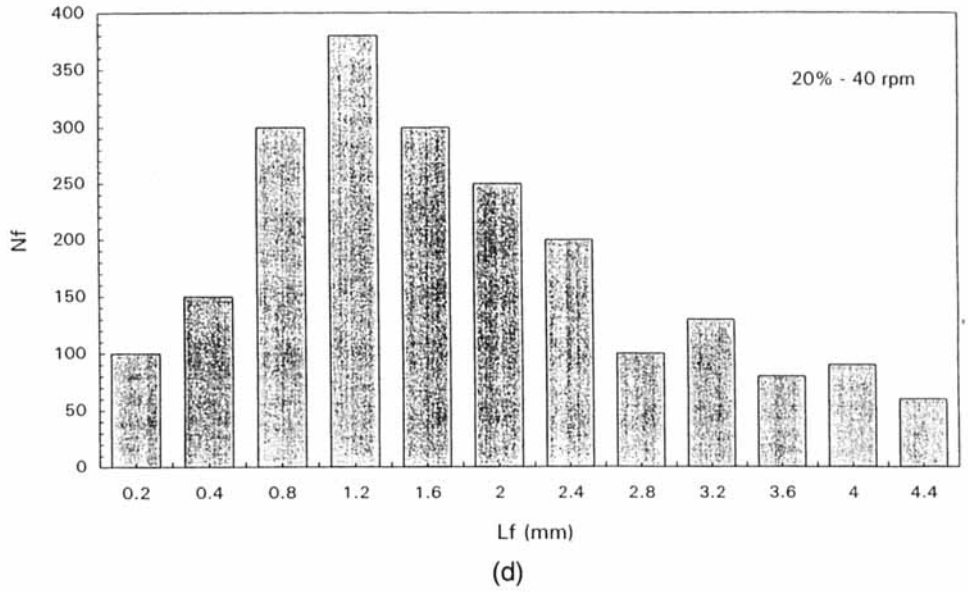

(d)

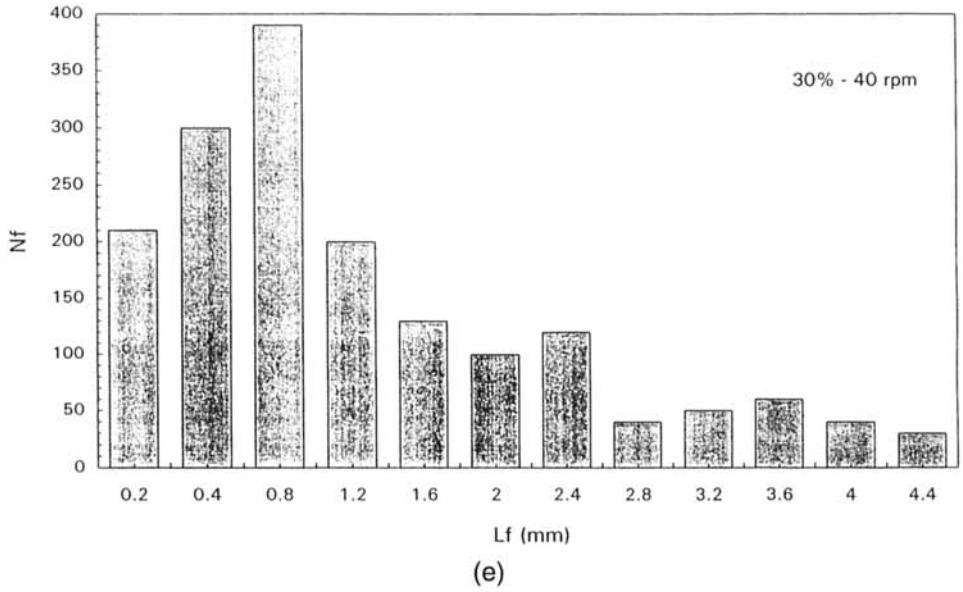

(e)

Fig. 8. Continued.

used to determine polymer molecular weight. The principal parameters are

$$L_n = \frac{\Sigma_i n_i L_i}{\Sigma_i n_i} \quad \text{is the average fiber length} \qquad (9)$$

$$L_w = \frac{\Sigma_i n_i L_i^2}{\Sigma_i n_i L_i} \quad \text{is the weight average length} \qquad (10)$$

$$P = \frac{L_w}{L_n} \quad \text{is the polydispersity index} \qquad (11)$$

This polydispersity index gives a method to measure the scatter or broadness of the fiber length distribution. Evidently, if P = 1, the system is monodisperse and values of P higher than 1 are expected in real cases. The fibers used in this study were monodispersed strands and the compound used to feed the extruder were prepared by gentle mechanical mixing (the integrity of the strands and fibers was verified after mechanical mixing). Then, it can be considered that the composite system is originally monodispersed with $L_n = L_w = 4.5$ mm and P = 1. The results of fiber length distributions obtained on different extruded specimens after processing are shown in *Tables 3* to *5* for the three variables analyzed: fiber concentration, capillary length, and extrusion rate, respectively. Although wide ranges of the three variables were

analyzed, results reported in these tables correspond in each case to changes in one variable, while the other two were fixed at an intermediate value.

Figures 8a to *8d* show the histograms of fiber length distributions for different fiber concentrations processed at 40 rpm. It should be noticed that, unlike previous studies (10–14), we have used monodispersed feeding systems; then, the final length distribution is a real measure of the breakdown of the fibers. The data reported shows that fiber breakdown increases with its concentration and that P decreases. Although these results are typically expected for these processes, they can be explained in terms of a more fundamental analysis. The principal cause of fiber attrition is mechanical breakdown by fiber-pellet interaction in the feeding section and fiber-fiber and fiber-metal interactions in the screw channel. In our case only the last effect must be considered as the resin was fed in powder form. The experimental results (*Table 4*) show that fiber breakdown was not a function of the die length, suggesting that most of fiber breaking occurs in the extruder barrel and not in the die. This fact confirms the observations of the orientation analysis which showed that, although their average length is greater than the capillary diameter, fibers are already oriented at the die entrance.

CONCLUSIONS

Rheological properties and morphological characteristics of glass fiber polypropylene composites have been measured and analyzed over a wide range of shear rates of practical interest for processing technologies. The viscosity shows a linear dependence with shear rate, fitted by a power-law equation, in good agreement with earlier studies. The irregularities in the extrudate surface increase with the fiber content and decrease with the shear rate. Fiber segregation increases with fiber content but it is not a function of the shear rate. Fiber alignment in the flow direction and orientation homogeneity across the filaments increase as fiber content decreases and shear rate increases. Average fiber length was drastically reduced during processing. Final fiber length appears to be independent of die length but decreases with fiber and shear rate.

The results of this research can allow a more rational definition of the processing conditions for the processing of short-fiber thermoplastic matrix composites and should be considered as the first step of a very extensive experimental and theoretical study of these materials.

ACKNOWLEDGMENTS

This research has been partially supported by the Italian National Research Council (CNR-Comitato Tecnologico) and by MURST. The contribution of the National Research Council of Argentina (CONICET) in the form of a fellowship granted to one of us (S. B.) is gratefully acknowledged.

REFERENCES

1. Jeffery, *Pro. Roy. Soc.*, **102**, 161 (1922).
2. R. G. Cox, *Pro. Roy. Soc.*, **14**, 284 (1971).
3. M. Kamal and A. Mutel, *Polym. Compos.*, **10**, 337 (1989).
4. E. Hinch and L. Leal, *J. Fluid Mech.*, **76**, 187 (1976).
5. S. Dinh and R. Armstrong, *J. Rheol.*, **29**, 905 (1985).
6. F. Folgar and C. Tucker III, *J. Reinf. Plast. Compos.*, **3**, 98 (1984).
7. M. Bibbo, S. Dinh, and R. Armstrong, *J. Rheol.*, **29**, 905 (1985).
8. S. E. Barbosa and M. A. Bibbo, *J. Appl. Polym. Sci: Appl. Symp.*, **49**, 127 (1991).
9. S. E. Barbosa, D. Ercoli, M. Bibbo, and J. Kenny, *Composite Structures*, **27**, 129 (1994).
10. L. A. Goettler, *Modern Plastics*, **47** (4),140 (1970).
11. P. F. Bright, R. J. Crowson, and M. J. Folkes, *J. Mat. Sci.*, **13**, 2497 (1978).
12. L. Czarnecki and J. White, *J. Appl. Polym. Sci.*, **25**, 1217 (1980).
13. B. Knuttson and J. White, *J. Appl. Polym. Sci.*, **26**, 2347 (1981).
14. M. Bercraft and A. Metzner, *J. Rheol.*, **36** (1), 143 (1992).
15. S. Middleman, in *Fundamentals of Polymer Processing*, McGraw-Hill, New York (1978).
16. M. Doi and S. Edwards, *J. Chem. Soc. Faraday Trans.*, **2**, 74, 560 (1978a).
17. M. Doi and S. Edwards, *J. Chem. Soc. Faraday Trans.*, **2**, 74, 918 (1978b).
18. G. K. Batchelor, *J. Fluid Mech.*, **46**, 813 (1971).
19. S. E. Barbosa, PhD Thesis, Universidad Nacional del Sur, Bahia Blanca Argentina (1992).
20. B. Hartmann and A. A. Haake, *J. Appl. Polym. Sci.*, **30**, 1553 (1985).
21. L. Utracki, *Polym. Compos.*, **7**, 284 (1986).